International Journal of Modern Manufacturing Technologies
ISSN 2067–3604, Vol. XIV, No. 3 / 2022
https://doi.org/ 10.54684/ijmmt.2022.14.3.239

PROPULSION THRUST FORCE CALCULATION WITH CAVITATION FOR AN UNDERWATER VEHICLE

Adrian Sabau, Ion Serbanescu, Remus Zagan

Constanta Maritime University, Faculty of Marine Engineering,
104 Mircea cel Batran Street, 900663, Constanta, Romania

Corresponding author: Ion Serbanescu, ion.serbanescu@cmu-edu.eu

Abstract: This paper aimed to evaluate the thrust force for a propeller taking into account cavitations, to analyze the dynamic and nautical characteristics of an ROV (Remotely Operated Vehicles). This approach is not a theoretical one, it also has a practical purpose to achieve high-performance propulsion systems with the lowest possible design costs. This is the purpose for which we want to create a viable and high-performance simulation model which allows optimization by numerical analysis, and in the end to make the prototype and perform measurements. The simulation is done in Ansys CFX and uses a 3D model for the propeller and duct of the T100 thruster produced by Blue Robotics. The simulation introduces the cavitation model from Ansys CFX, simplified Rayleigh-Plesset formulation, and we will perform analyses whit important improvements. Taking into account the results obtained in previous author work [1] and information from other scientifical papers, we will test fine discretization mesh in rotor zone to solve the cavitation. Increased resolution for the numerical scheme, two-order schemes for pressure momentum, and turbulence equations. Replacement of k-epsilon turbulence model whit a more performant k-omega model. The obtained results will be analyzed and compared with the experimental measurements.

Key words: cavitation, thrust force, rotating frame, stationary domain, momentum equation, numerical scheme resolution.

1. INTRODUCTION

The present paper is an improvement of an older one [1] which aimed to evaluate the thrust force for an ROV (Remotely Operated Vehicles, vehicles that are operated underwater and remotely) to analyse the dynamic and nautical characteristics. At the first time, only a general evaluation of the thrust characteristics was done. At this time a more detailed calculation will be done, whit more efficient calculation models that will take into account as many factors as possible, to obtain a high-performance model (in accordance whit hardware capability) that later can be used to optimize the propulsion system. Measuring the characteristics of a propulsion system is not very difficult, but the costs of making various propeller variants are very high. This is the purpose for which we want to create a viable and high-performance simulation model which allows optimization by numerical analysis, and in the end to make the prototype and perform measurements.

The first simulation was performed using Ansys CFX software. The results obtained at that time were satisfactory only at low speeds, for the field of high speeds (specific to ROV propeller) the results were not very precise. After a thorough analysis, the most important conclusion was that the cavitation effect was not taken into account.

The effects of cavitation have been studied by various authors in detail on ship propellers, [2, 3] which operate at low speeds and the results are promising. For duct thrusters, running at high speeds (like this one) [4], the results are not as good. The multiphase approach imposed by cavitation (mixture of water and vapours) raises multiple issues both numerically and hardware. After a thorough documentary study, in this paper, the author mainly aims to introduce the Rayleigh-Plesset cavitation model in the simulation and replace the standard k-ε turbulence model whit the Shear Stress Transport model an improved variant of the k-ω model whit know good performance in a rotational domain.

2. THEORETICAL APPROACH

The theoretical model used is mainly the one currently used to solve this type of problem [4]. The introduction of cavitation into the study requires the use of the multiphase approach for a compressible flow. For cavitating flow modelling, an isothermal, Eulerian-Eulerian, homogeneous multiphase model is typically used. The tendency for a flow to cavitate is characterized by the cavitation number, defined as:

$$C_c = \frac{p - p_v}{\frac{1}{2} r U_m^2} \quad (1)$$

where p [Pa] is a reference pressure for the flow, p_v [Pa] is the vapor pressure, U_m [m/s] mean speed and the remaining term represents the dynamic pressure. In the simplified cavitation models, mass transfer is achieved by mechanical effects, namely liquid-vapor pressure differences.

Ansys CFX implements the Rayleigh Plesset model in the multiphase domain as an interphase mass transfer model. The Rayleigh-Plesset equation provides the basis for rate controlling of vapor generation and condensation. The model base equation represents the growth of vapor bubble:

$$R_B \frac{d^2 R_B}{dt} + \frac{3}{2}\left(\frac{dR_B}{dt}\right)^2 + \frac{2\sigma}{\rho_f R_B} = \frac{p_v - p}{\rho_f} \qquad (2)$$

where R_B[m] is the radius of the vapor bubble, σ[N/m] is the surface tension between the vapor and liquid, and ρ_f [kg/m^3] is the density of the liquid. After simplifications and rearrangement of terms, the total interphase mass transfer rate per unit volume in the evaporation process is:

$$\dot{m}_{fg} = N_B \frac{dm_B}{dt} = \frac{3 r_g \rho_g}{R_B}\sqrt{\frac{2}{3}\frac{p_v - p}{\rho_f}} \qquad (3)$$

where N_B, r_g is the number of gas bubbles and the volume fraction of gas per unit volume and ρ_g [kg/m^3] is the density of the gas. Since cavitation requires the simultaneous approach of evaporation and condensation, equation (3) is written as follows:

$$\dot{m}_{fg} = F\frac{3 r_g \rho_g}{R_B}\sqrt{\frac{2}{3}\frac{|p_v - p|}{\rho_f}}\, sign(p_v - p) \qquad (4)$$

where F is an empirical factor that differentiates condensation and evaporation processes that have different unfolding speeds, condensation is slower. On the other side, vaporization is initiated by the nucleation centres (microparticles or bubbles of non-condensed gases). For numerical modelling, the bubble radius R_b is replaced by the nucleation site radius R_{nuc} and volume fraction of gas by r_g by $r_{nuc}(1-r_g)$ relation, r_{nuc} volume fraction of the nucleation sites. In this condition equation (4) is rewritten as and this is source term on the homogeneous multiphasic flow model:

$$\dot{m}_{fg} = F\frac{3 r_{nuc}(1-r_g)\rho_g}{R_{nuc}}\sqrt{\frac{2}{3}\frac{|p_v - p|}{\rho_f}}\, sign(p_v - p) \qquad (5)$$

Ansys CFX, Rayleigh Plesset cavitation model uses the following implicit parameters: $Rnuc$=1 μm, r_{nuc}=5.0e-4, F_{evap}=50, F_{cond}=0.01,

For flow modelling, we use a compressible, isothermal, Eulerian-Eulerian, homogeneous multiphase model. This approach makes the approximation that the speeds of the two phases $U_f=U_g=U$ (liquid and vapours) are equal; which are in good agreement whit the reality in the case of cavitation phenomena.

The system of equations of the model are [4]:

- Continuity equation:

$$\begin{aligned} \frac{\partial}{\partial t}(r_f \rho_f) + \nabla(r_f \rho_f U) &= \dot{m}_{fg} \\ \frac{\partial}{\partial t}(r_g \rho_g) + \nabla(r_g \rho_g U) &= \dot{m}_{fg} \end{aligned} \qquad (6)$$

- Momentum equation:

$$\frac{\partial}{\partial t}(\rho U) + \nabla(\rho(UU) - \mu(\nabla U + (\nabla U)^T)) = -\nabla p \qquad (7)$$

$$\begin{aligned} \rho &= r_f \rho_f + r_g \rho_g \\ \mu &= r_f \mu_f + r_g \mu_g \\ p &= p_f = p_g \end{aligned} \qquad (8)$$

The homogeneous multiphase equation is similar to whit momentum transport equation in a single phase and interphase transfer terms have all been cancelled.

- Transport equation for turbulence model k-ω, Shear Stress Transport (SST) formulation:

$$\frac{\partial(\rho k)}{\partial t} + \frac{\partial(\rho k U_j)}{\partial x_j} = \frac{\partial}{\partial x_j}\left[\left(\mu + \frac{\mu_t}{\sigma_k}\right)\frac{\partial k}{\partial x_j}\right] + P_k - \beta' \rho k \omega \qquad (9)$$

$$\frac{\partial(\rho\omega)}{\partial t} + \frac{\partial(\rho U_j \omega)}{\partial x_j} = \frac{\partial}{\partial x_j}\left[\left(\mu + \frac{\mu_t}{\sigma_{\omega 1}}\right)\frac{\partial \omega}{\partial x_j}\right] + (1-F_1)2\rho\frac{1}{\sigma_{\omega 2}\omega}\frac{\partial k}{\partial x_j}\frac{\partial \omega}{\partial x_j} + P_\omega - \beta_2 \rho \omega^2 \qquad (10)$$

$$\mu_t = \rho\frac{k}{\omega}, \quad \nu_t = \frac{\alpha k}{\max(\alpha\omega SF_2)}, \quad \nu_t = \frac{\mu_t}{\rho}, \quad P_\omega = \left(\frac{\alpha_2}{\nu_t}\right)P_k, \quad \sigma_k = 1.176,$$
$$\sigma_{\omega 1} = 2, \quad \beta' = 0.09, \quad \alpha_1 = \frac{5}{9} \quad \alpha_2 = 0.44, \quad \beta = 0.0828, \quad \sigma_{\omega 2} = \frac{1}{0.856} \qquad (11)$$

where P_k, P_ω represents the generation of turbulence kinetic energy (k), turbulent frequency (ω due to the mean velocity gradients, σ_k, σ_ε are the turbulent Prandtl numbers, μ_t is turbulent viscosity and F_1, F_2 is a specific blending function, υ_t is a limiter to the

formulation of the eddy-viscosity and S is an invariant measure of the strain rate.
The calculation is done running a steady-state analysis, using a simplex algorithm, whit pressure corrections and high-resolution option for advection schemes and turbulence numeric.

3. PROGRAM SETTINGS

The simulation uses a 3D model of an asymmetrical propeller in the duct, imported from a previous paper [1] having as reference the BlueRobotics's T100 propeller presented in Figure 1. The mesh is also imported from the previous work but needs adjustments due to hardware limitations. The 1.3 million previously obtained network elements are impossible to use with the much more complex new model, the CFX solver runs only in RAM memory.
The maim fluid domain is decomposed in two fluid sub-domains, one is static and the next around the propeller is rotating whit constant speed, in the interval 0-4350 rpm around the z-axis. The two sub-domains were defined as homogeneous multiphase fluid domains, both consisting of water and water vapor at 25 ° C with interphase mass transfer generated by cavitation, modelled with Rayleigh-Plesset relationships and 3137 Pa, water vapor saturation pressure at 25°C. Both domains are initialized with 1 atm as a reference pressure and 0% water vapor concentration. For each subdomain, the turbulence model set is the SST Shear Stress Transport model, an improved variant of the k-ω model.
The boundary condition was set (Figure 2):
- Inlet – imposed total pressure, normal flow direction, and medium turbulence (5%)
- Outlet – imposed average relative static pressure, whit pressure blended profile 0.05.
- Wal - is set as implicit no-slip, smooth roughness

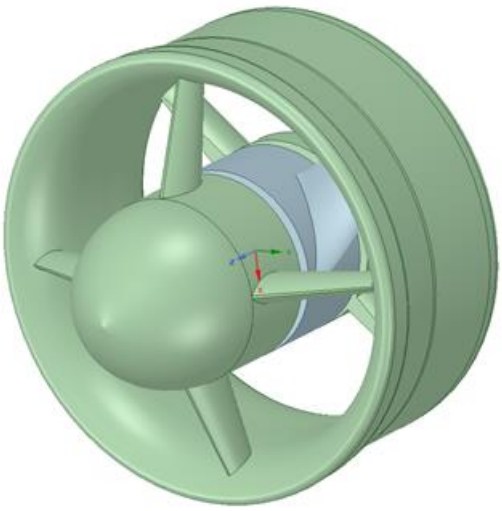

Fig. 1. The 3D model of T100 thruster

The interface for this problem was chosen "General Connection". To reduce the computational time and memory usage "Frozen rotor" was set whit "Specified pitch angles" as a condition. This model requires the least amount of computational effort and is accurate when steady-state calculations are done.
For numerical solutions "High order" advection scheme is set for continuity, momentum, and turbulence equations.

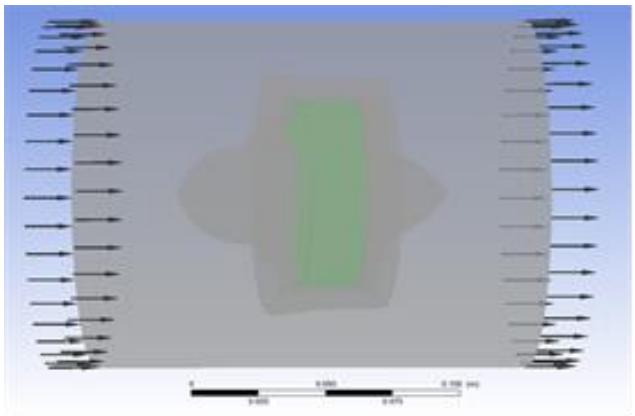

Fig. 2. Boundary condition

The working model and calculation cases have been dimensioned taking into account the computational hardware resource, RAM memory, and computer time. All the case calculations are done integral in the computer RAM memory, without performing write operations on disk, only in case of saving the data, this is a mandatory condition for Ansys CFX solver.

4. SIMULATION RESULTS

The first time we need to calibrate the discretization network. The very fine discretization network used in the calculation without cavitation [1] cannot be used with the new model due to hardware limitations. For this reason, we perform a network calibration calculation using the cavitation model. At 2000 rpm the limit speed at which the no-cavitation model also provided satisfactory results [1]. After successively reducing the fineness of the network, it reached 1 million cells. Taking advantage of the fact that the model has two domains, they were discretized with different degrees of fineness, higher for the central rotational area where the cavitation develops and smaller for the stationary network area. The resulting network is shown in figure 3.
Modifying only rotational speed in the interval 0-4350 rpm, we have done calculations. For the ROV operating the 300 and 1000 rpm speed is tow steps manoeuvring speed and for moving we use tow step 2000 and 3000 rpm speed, maximum propulsion speed is 4350 rpm. The solution was obtained under stationary, isothermal, conditions using flow equations (continuity and moment) cavitation model and tow turbulence model standard k-ε

model and k-ω SST model. The computational time was approximately 8 hours for each case whit k-ε model and 20 hours for k-ω SST.

The selected representative results are presented in figures 4 to 11. The rotational speed selected is the maximum propulsion and manoeuvring speed representative for ROV functionality, 4200 rpm is the maximum speed, 1000 rpm is the maximum manoeuvring speed and 3000 rpm is the cruise speed.

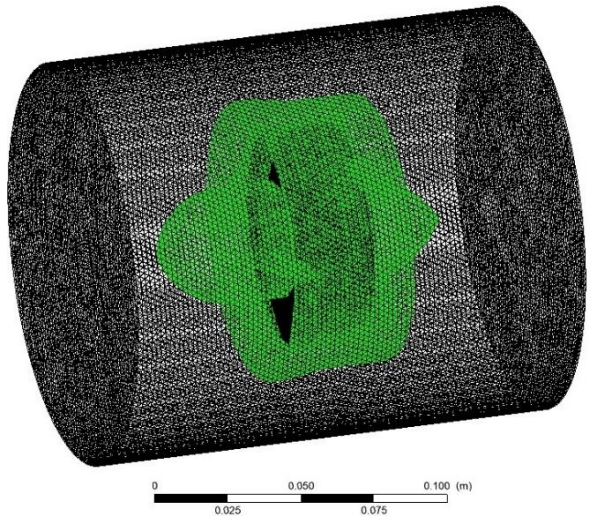

Fig. 3. Mesh, 1 million cells

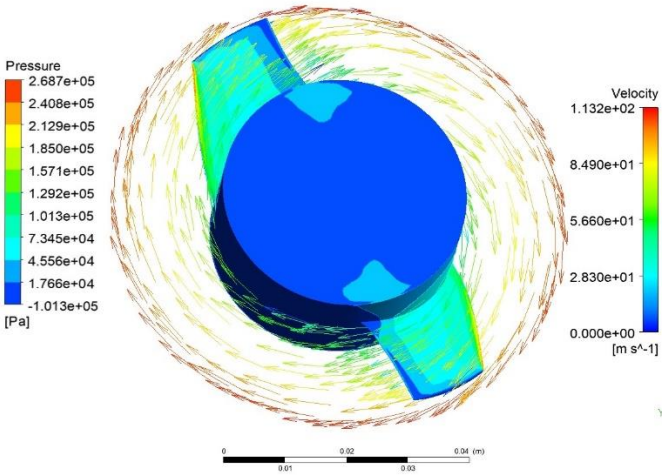

Fig. 4. Mesh, 1 million cells

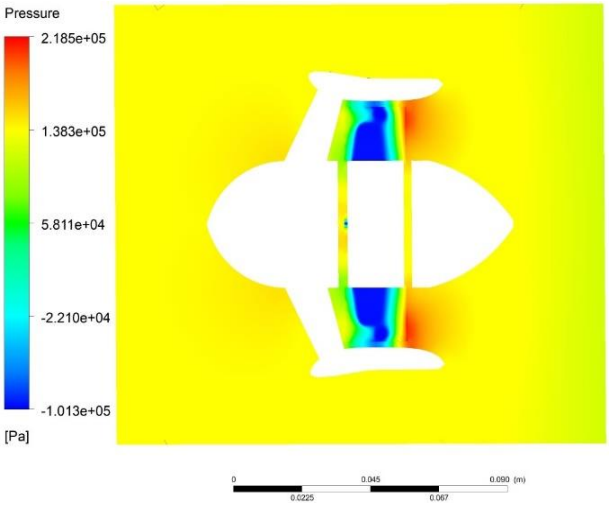

Fig. 5. Pressure at 3000 rpm

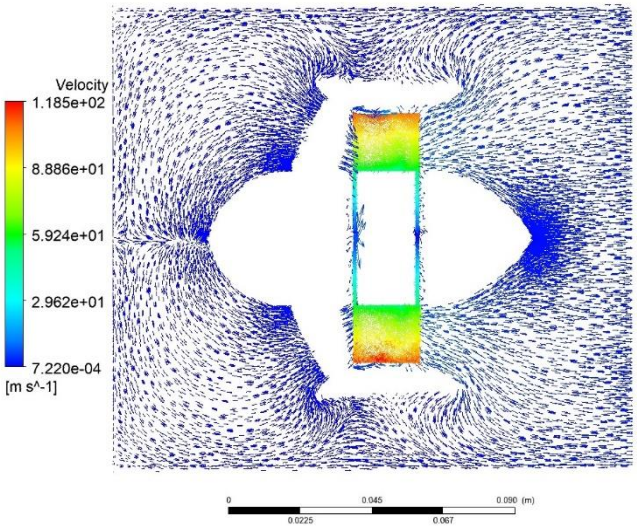

Fig. 6. Velocity at 1000 rpm, k-ω SST model

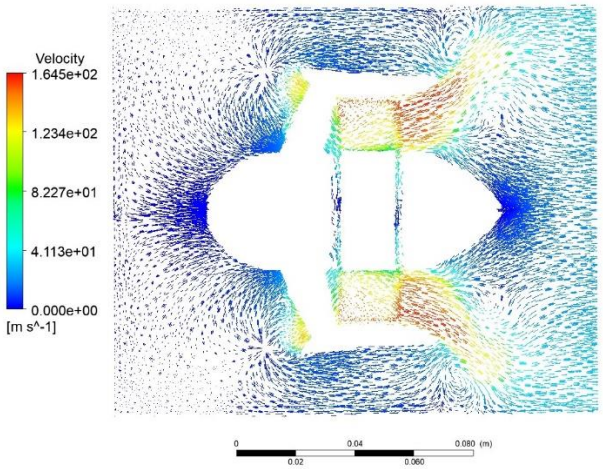

Fig. 7. Velocity at 3000 rpm, k-ω SST model

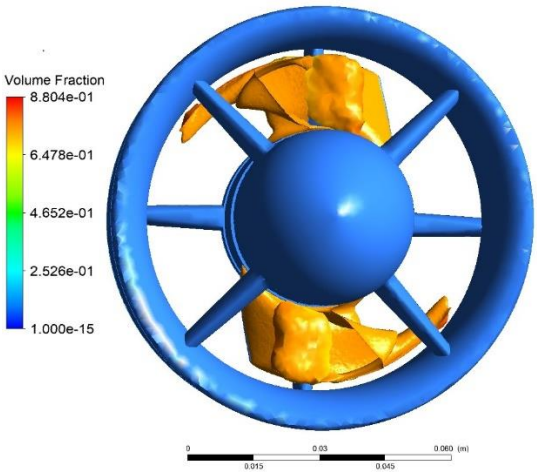

Fig. 8. Vapor fraction at 4350 rpm, k-ω SST model

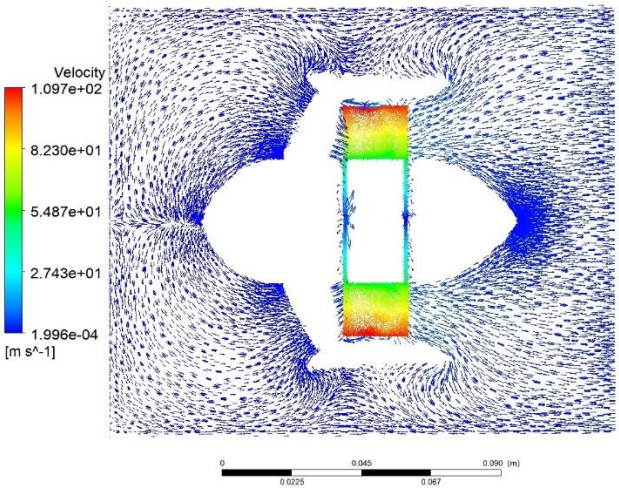

Fig. 9. Velocity at 1000 rpm, k-ε model

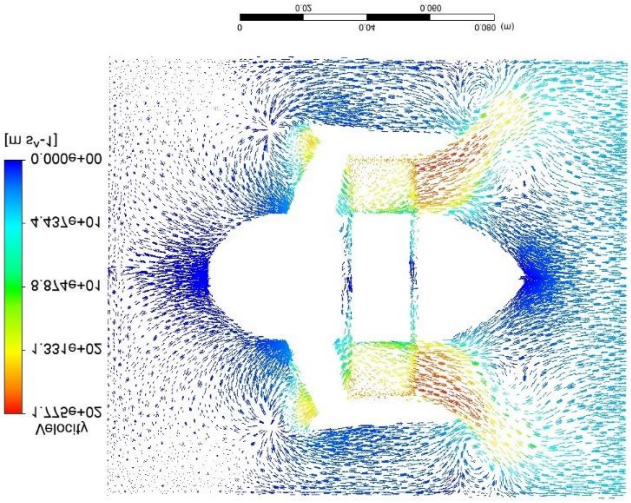

Fig. 10. Velocity at 3000 rpm, k-ε model

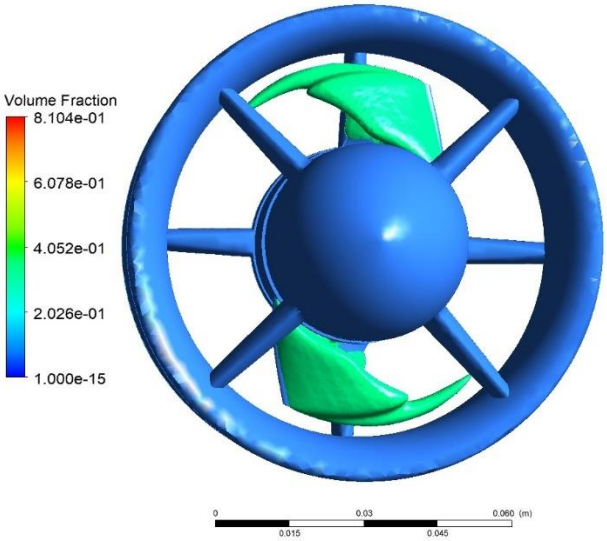

Fig. 11. Vapor fraction at 4350 rpm, k-ε model

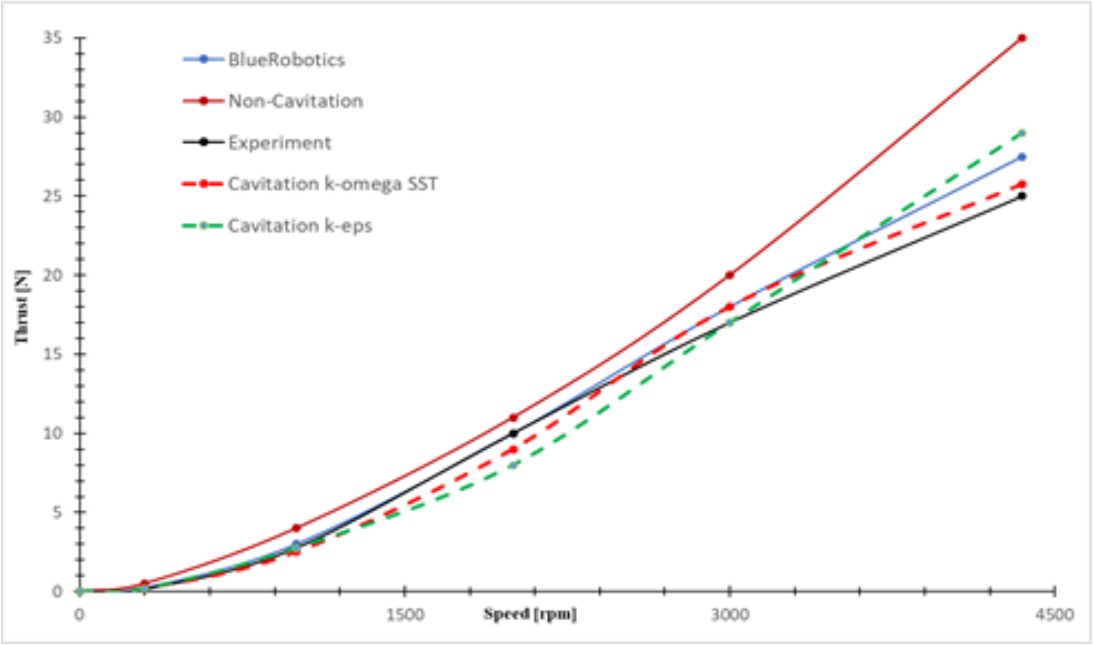

Fig. 12. Propeller thrust force characteristic

In the end, using the facilities of the program, the thrust force of the propeller was calculated for a single direction of rotation, the propeller. The calculation results and the comparison with the experimental data available are presented in Figure 12.
The experimental data used in the study come from two sources, one from the BlueRobotics and the other our measurements made in the hydrodynamic testing basin of the University [1]. The results obtained from the two sources were filtered and interpolated [5] and the comparative results are shown in Figure 12.

5. CONCLUSIONS

The graph in figure 12 presents the results after simulation. We can be concluded that the simulation whit cavitation can provide whit a good approximation of the thrust force generated by propellers, and thus the main goal of this work was achieved.
The cavitating model whit k-ω SST model offered the best approximation, as we are expected, generate by the superior characteristic of the turbulence model. The standard k-ε model has known difficulties to simulate the correct turbulent regime in rotational domain.
Bott model generates under estimation an overestimation of thrust force in the same region, most probably due to the incorrect estimation of the turbulent regime.
Future improvements should replace the turbulent models with more powerful ones, but this also requires a major upgrade of the hardware, at least more available memory, RAM.

6. ACKNOWLEDGMENTS

The authors are grateful for funding the publication of research from the project CNFIS-FDI-2022-0639 with title MCU- international landmark of excellence in maritime education and research.

7. REFERENCES

1. Sabau, A., (2020). *Thrust force evaluation for an ROV (Remount Operating Vehicle) propeller*, IOP, Material Science and Engineering, 916, 012098.
2. Pereira, F., Salvatore, F., Felice, F., (2004). *Measurement and Modelling of Propeller Cavitation in Uniform Inflow*, Journal of Fluids Engineering, 126, 671–679.
3. Scurtu, I.C., Panaitescu, V.N., (2019). *Turbulent Flow Numerical Simulation for Unconventional Propulsion*, Revista de Chimie, 70(10), 3508-3511.
4. Jie, G., Jiangming, D., Lianzhou, W., (2021). *Propeller–duct interaction on the wake dynamics of a ducted propeller*, Physics of Fluids, 33, 074102.
5. Oanta, E., Danisor, A., Tamas, R., (2016). *Study regarding the spline interpolation accuracy of the experimentally acquired data*, Proc. SPIE 10010, Advanced Topics in Optoelectronics, Microelectronics, and Nanotechnologies VIII, 1001007.

Received: April 17, 2022 / Accepted: December 15, 2022 / Paper available online: December 20, 2022 © International Journal of Modern Manufacturing Technologies